Reactions of Dienes with the Ion $[Ir(PPh_3)_2(OCMe_2)_2H_2]^+$: A Kinetic and Mechanistic Study of Complex Formation and Diene Hydrogenation

Oliver W. Howarth, Colin H. McAteer, Peter Moore,* and George E. Morris
Department of Chemistry and Molecular Sciences, University of Warwick, Coventry CV4 7AL

Stopped-flow n.m.r. reveals markedly different rates of co-ordination of cyclo-octa-1,5-diene (cod) and bicyclo[2.2.1]hepta-2,5-diene (norbornadiene, nbd) to the ion $[Ir(PPh_3)_2(OCMe_2)_2H_2]^+$ (1). $[Ir(PPh_3)_2(diene)H_2]^+$ ions are the first formed products. The interconversion of all three $[Ir(PPh_3)_2(nbd)H_2]^+$ isomers has been observed by ^1H and ^{31}P n.m.r. spectroscopy. These species react further to give $[Ir(PPh_3)_2(nbd)]^+$ (2), either by H_2 elimination, or by hydrogenation of the co-ordinated nbd to form bicyclo[2.2.1]hept-2-ene (norbornene, nbe). Stopped-flow spectrophotometry reveals a marked inverse kinetic isotope effect for the formation of (2) during the hydrogenation or deuteriation of nbd. A mechanism involving an equilibrium between diene–dihydride and alkyl–hydride is proposed. The dienes 2,3-dimethylbutadiene and cyclohexa-1,3- or -1,4-diene react with (1) to give highly fluxional allyl–hydride species which feature an aliphatic C–H $\cdots$ Ir^{III} interaction. Variable-temperature ^1H and ^{31}P n.m.r., and ^1H spin-saturation transfer experiments reveal a facile reversible hydrogen-transfer process between metal and hydrocarbon ligand which occurs *via* a C–H $\cdots$ Ir^{III} interaction.

Cationic bis(phosphine)iridium complexes such as $[Ir(PR_3)_2(cod)]^+$ (cod = cyclo-octa-1,5-diene; R_3 = Pr^i_3, Ph_3, or $MePh_2$),[1,2] or the acetone solvate $[Ir(PPh_3)_2(OCMe_2)_2H_2]^+$ (1),[3] are active catalyst precursors for the hydrogenation and isomerisation of alkenes in dichloromethane solution. Although alkene–dihydride species are often proposed as intermediates in these processes, they are rarely observed. However, they have been characterised during the hydrogenation of cod by $[Ir(PPh_3)_2(cod)]^+$. Thus two diene–dihydride isomers of $[Ir(PPh_3)_2(cod)H_2]^+$ have been observed in CD_2Cl_2 by low-temperature ^1H n.m.r.[4] The first isomer, structurally analogous to (3a), is formed by substitution of the acetone molecules of (1) by cod. The second, structurally analogous to (3c), is formed by the *cis*-addition of H_2 to $[Ir(PPh_3)_2(cod)]^+$. It is interesting to note that these isomers have not been reported to interconvert. More recently, Crabtree *et al.*[5] have demonstrated that (1) may also dehydrogenate cycloalkanes under mild reaction conditions especially in the presence of t-butylethene. This is the first *bona fide* example of an intermolecular sp^3 C–H bond cleavage of a non-activated alkane substrate by a soluble transition metal species, although other examples have been reported since.[6]

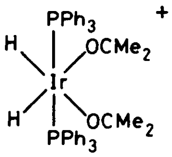

(1)

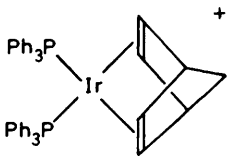

(2)

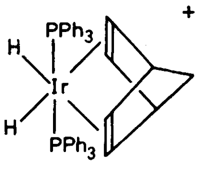

(3a)

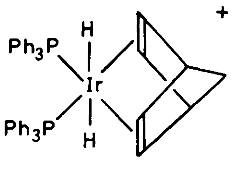

(3b)

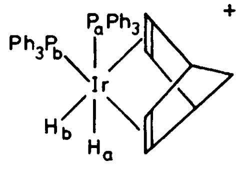

(3c)

The ability of (1) to catalyse the hydrogenation of alkenes, and to dehydrogenate cycloalkanes, must in part be due to the ease with which acetone is displaced from the iridium(III) centre. We have previously shown that solvent exchange with cations of the type $[M(PR_3)_2(solvent)_2H_2]^+$ (M = Rh^{III} or Ir^{III}, R = Ph or C_6H_{11}, solvent = MeCN or Me_2CO) occurs *via* a dissociative *D* mechanism, leading to a transient five-co-ordinate species.[7] This study revealed that a large variation in the $\Delta H^\ddagger$ values for solvent exchange could explain the major differences between the acetone and acetonitrile solvates. The $\Delta H^\ddagger$ values are 67 and 96 kJ mol^{-1} for solvent exchange with (1) and $[Ir(PPh_3)_2(NCMe)_2H_2]^+$, respectively. Thus, the catalytically active acetone solvate is some 10^5 times as labile as its acetonitrile analogue, which itself shows minimal hydrogenation activity. We have recently shown that only the labile acetone solvates react with organometallic Lewis bases. Thus, $[Ir(PPh_3)_2(NCMe)_2H_2][PF_6]$ does not react with $[W(\eta^5\text{-}C_5H_5)_2H_2]$, whereas (1) does to give the alkyl–hydride species $[(PPh_3)_2HIr(\mu\text{-}H)_2(\mu\text{-}\sigma : 1\text{—}5\text{-}\eta\text{-}C_5H_4)W(\eta^5\text{-}C_5H_5)][PF_6]$.[8] An intermediate which quickly forms during this reaction has been characterised as the acetone-substituted species, $[(PPh_3)_2H_2Ir(\mu\text{-}H)_2W(\eta^5\text{-}C_5H_5)_2]^+$. The slower second stage of this reaction involves insertion into the η^5-cyclopentadienyl C–H bond and reveals a deuterium isotope effect.[9]

We now report in full our studies concerning the reactions of (1) with dienes. The results are divided into three sections: (*i*) the binding of cod and bicyclo[2.2.1]hepta-2,5-diene (norbornadiene, nbd) to (1) as studied by stopped-flow (s.f.) n.m.r.;[7,10–12] (*ii*) the subsequent rearrangements of the diene dihydrides involved in the nbd reaction, leading to hydrogenation and the formation of bicyclo[2.2.1]hept-2-ene (norbornene, nbe); and (*iii*) the detection of highly fluxional allyl–

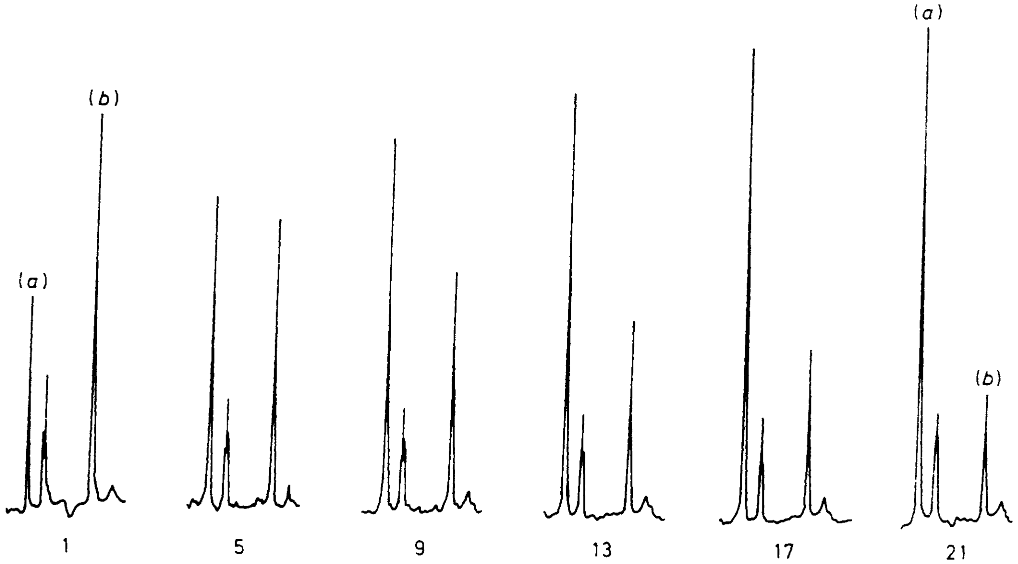

Figure 1. Parts of successive 90-MHz ^1H n.m.r. spectra obtained by s.f. n.m.r. $[(1)] = 2.45 \times 10^{-2}$, $[nbd] = 7.6 \times 10^{-2}$ mol dm^{-3}, CD_2Cl_2 solution at 233.3 K: (*a*) free Me_2CO at δ 2.16 p.p.m.; (*b*) co-ordinated Me_2CO at δ 1.41 p.p.m. The initial free Me_2CO concentration was 6.7×10^{-3} mol dm^{-3}. The poorly resolved triplet between the two Me_2CO resonances arises from the methylene protons of free nbd

hydride species which feature an aliphatic $C-H \cdots Ir^{III}$ interaction. Parts of this work have appeared in two previous communications.[13,14]

Results and Discussion

Stopped-flow N.M.R. Diene Binding Studies.—The rate of diene substrate binding to the solvated iridium ion (1) was monitored in a s.f.n.m.r. experiment, by following the decay of the co-ordinated acetone resonance (δ 1.41 p.p.m.) with time, in a manner similar to that described previously.[7,10-12] A small amount of $SiMe_4$ was added as a reference signal (used for normalising spectra), together with the relaxing agent tris(acetylacetonato)chromium(III) (2×10^{-3} mol dm^{-3}) to minimise spin-saturation effects. A typical set of s.f.n.m.r. spectra obtained for nbd binding to (1) at 233.3 K is shown in Figure 1. The half-life for the reaction with nbd is *ca.* 10 s at this temperature, whereas under the same conditions the half-life for the reaction with cod is 30 min. Above 233.3 K, the nbd reaction becomes too fast to monitor by s.f.n.m.r., although the cod reaction could be followed even at 265 K.

The proposed reaction mechanism for diene substrate binding is shown in Scheme 1 [$S = Me_2CO$, $M = Ir(PPh_3)_2H_2^+$]. This scheme allows for solvent exchange at (1) *via* a dissociative *D* mechanism,[7] and includes a mono-bound diene species II as an intermediate. Monoene species have been observed in equilibrium with (1) at similar temperatures and concentrations, using cyclo-octene or styrene.[7] However, the monoene complexes are far less stable, and incomplete formation is observed even in the presence of a ten-fold excess of monoene. Complete acetone displacement occurs with dienes, highlighting a marked chelate effect. No mono-bound cod could be detected by ^1H n.m.r. during its binding, and although a small amount of mono-bound nbd species is initially observed, it is believed to be the *exo*-bound species [structure (4)] and its presence will have minimal effect on the kinetic treatment presented here.

Applying the steady-state approximation to the intermediates I and II in Scheme 1 gives the rate law for diene-dihydride formation shown in equation (i) (see Appendix 1).

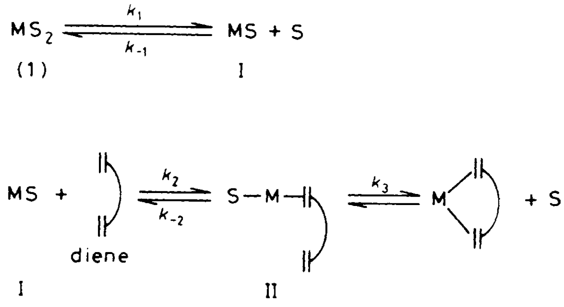

Scheme 1.

The only rate constant in Scheme 1 which can be obtained independently is k_1. This corresponds to the acetone exchange rate constant, and is calculated to be 0.153 s^{-1} at 233.3 K from the activation parameters.[7] The remaining rate constants (k_{-1}, k_2, k_{-2}, and k_3) cannot easily be separated, and are best collected in one term [A in equation (ii)]. The s.f.n.m.r.

$$\text{Rate} = \frac{k_1 A[MS_2][\text{diene}]}{[S] + A[\text{diene}]} \qquad \text{(i)}$$

$$\text{where } A = k_2 k_3 / k_{-1}(k_{-2} + k_3) \qquad \text{(ii)}$$

kinetic data were treated according to equation (A8) in Appendix 1, and Figure 2 shows a resulting rate plot for the nbd reaction. This treatment allows the determination of A for both dienes. Thus at 233.3 K, $A = 0.578 \pm 0.016$ for nbd and $(5.96 \pm 0.37) \times 10^{-4}$ for cod.

The considerably different diene substrate binding rates may be rationalised by the following considerations. For the rigid nbd molecule, the chelate ring closure step in Scheme 1 is likely to be fast compared with the rate of loss of nbd (*i.e.* $k_3 \gg k_{-2}$) and equation (ii) reduces to equation (iii). This

$$A \simeq k_2/k_{-1} \simeq 0.578 \pm 0.016 \qquad \text{(iii)}$$

implies that the rate of reaction depends on the ability of the five-co-ordinate monosolvate species I to discriminate between nbd and acetone, a preference being shown for the less hindered solvent molecule. In contrast to nbd, cod is a flexible cyclic diene. This will have important consequences upon the fate of the mono-bound diene species II in Scheme 1. Since considerable rearrangement of the cod methylene backbone is required before a favourable conformation is obtained for chelate ring closure, it seems likely that mono-bound cod dissociation occurs faster than the chelation reaction (*i.e.* $k_{-2} \gg k_3$). In this case equation (ii) will approach the alternative extreme condition (iv). If we assume that the k_2 values for

$$A \simeq k_2k_3/k_{-1}k_{-2} \simeq (5.96 \pm 0.37) \times 10^{-4} \qquad \text{(iv)}$$

the reaction of (1) with cod and nbd are very similar (*i.e.* similar rates of first bond formation during the reaction of different dienes with the five-co-ordinate intermediate), it can be estimated from equations (iii) and (iv) that $k_{-2} \simeq 970k_3$. This suggests that loss of cod from II is considerably faster than the rate-determining chelate ring-closure step at this temperature. This is consistent with the observed instability of monoene complexes (*i.e.* large k_{-2} values). The variation of the observed pseudo-first-order rate constants ($k_{obs.}$) with temperature for the reaction of cod with (1) is shown in Table 1. The activation parameters obtained from these data are $\Delta H^{\ddagger} = 89.1 \pm 4.4$ kJ mol^{-1} and $\Delta S^{\ddagger} = +74.2 \pm 17.7$ J K^{-1} mol^{-1}. As the $k_{obs.}$ values are a composite of several factors, the derived activation parameters are not directly interpretable, although they do allow the rate of reaction to be estimated at other temperatures.

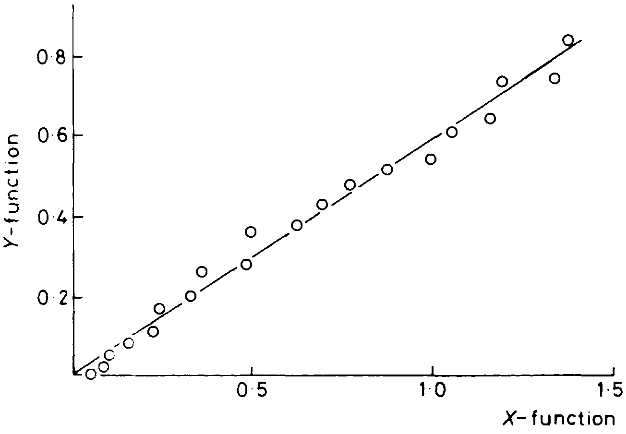

Figure 2. Least-squares plot, according to equation (A8), for the s.f.n.m.r. reaction of $[Ir(PPh_3)_2(OCMe_2)_2H_2][PF_6]$ (1) (2.45×10^{-2} mol dm^{-3}) and nbd (7.6×10^{-2} mol dm^{-3}) in CD_2Cl_2 at 233.3 K

Mechanism of nbd Hydrogenation Catalysed by (1).—The addition of nbd to a colourless solution of (1) in CD_2Cl_2 at room temperature leads to the rapid formation of the dark red square-planar iridium(I) species, $[Ir(PPh_3)_2(nbd)]^+$ (2). The main n.m.r. parameters for (2) are collected in Table 2. In addition to the formation of (2), hydrogenation occurs to form the monoene, norbornene (nbe). This is clearly demonstrated in the ^{13}C n.m.r. spectrum where resonances appear at δ 135.4 ($C^{2,3}$), 48.8 ($C^{1,4}$), 42.0 (C^7), and 24.8 p.p.m. ($C^{5,6}$), which is identical to an authentic sample of nbe. Confirmation that hydrogenation occurs exclusively at carbons 5 and 6 is obtained from the reaction of nbd with $[Ir(PPh_3)_2(OCMe_2)_2D_2][PF_6]$, $[^2H_2]$-(1). {For the assignment of the carbon resonances see the structure of $[^2H_2]$nbe, (5)}. Thus, the nbe carbon resonances are as before except that at δ 24.8 which collapses into a triplet due to deuterium coupling ($^1J_{CD}$ = 20.6 Hz). The ^1H n.m.r. spectrum of $[^2H_2]$nbe shows the absence of an nbe resonance at δ 0.84. This may be compared with a previous literature report [15] indicating that *cis*-addition occurs giving the *endo,endo*-5,6-dideuterionorbornene product as shown. The same product is also formed in the catalytic hydrogenation of nbd by $[Rh(PPh_3)_2(diene)]^+$ in acetone.[16] Integration of the ^1H n.m.r. spectra reveals the yield of nbe is less than that for (2) even with a 20-fold excess of nbd over (1). Thus, the initially formed $[Ir(PPh_3)_2(nbd)H_2]^+$ (3) species may form (2), either by the hydrogenation reaction in the presence of excess nbd, or by dihydrogen elimination. The analogous reaction between (1) and excess cod gives $[Ir(PPh_3)_2(cod)]^+$ with only a trace of cyclo-octene (as determined by ^{13}C n.m.r.), and H_2 elimination is by far the dominant pathway.

Unlike the reaction of cod with (1), where only one diene-dihydride transient is observed,[4] the nbd reaction is more complicated. Although s.f.n.m.r. reveals the first formed diene–

Table 1. Stopped-flow n.m.r. pseudo-first-order rate constants obtained for the reaction of (1) (2.5×10^{-2} mol dm^{-3}) and cod (0.25 mol dm^{-3}) in CD_2Cl_2 solution

T/K	$10^4k_{obs.}$/s^{-1}
264.7	939 ± 93
254.3	253 ± 17
243.7	30.1 ± 1.4
233.3	3.93 ± 0.28

Table 2. Selected n.m.r. data (δ/p.p.m.) for the bis(phosphine)iridium species involved in the nbd reaction at 223 K in CD_2Cl_2 solution [a]

	^{1}H N.m.r.					
Species	HC=CH	CH	CH_2	hydride	^{31}P N.m.r.	^{13}C N.m.r.
(1)	—	—	—	−27.6(t, 15.4)	27.8	
(2)	6.74	3.55	1.92	—	21.6	70.8(t, 4.6), [b] 71.5(t, 4.6) [b] 51.7
(3a)	4.01	3.22	0.59	−15.9(t, 16.5)	4.2	67.5, 65.4, 46.8
(3b)	2.95	3.85	0.59	−7.7(t, 17.6)	13.0	
(3c)				H_a −10.1(ddd, 84.7, 21.5) H_b −14.2(ddd, 22.3, 13.4) ($^2J_{HH}$ = 5.5)	P_b 13.4(d) P_a −5.1(d) ($^2J_{PP}$ = 17.6)	
(4)				−11.1(t, br, 14.1) −29.5(t, br, 14.1) ($^2J_{HH}$ unresolved)	15.4	

[a] Coupling constants (Hz) are in parentheses. [b] Pseudo-triplets due to virtual coupling.

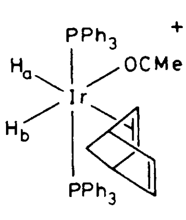

(4)

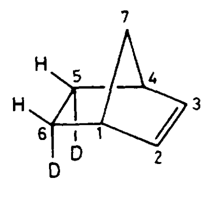

(5)

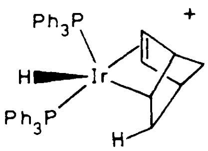

(6)

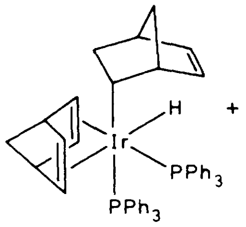

(7) = X

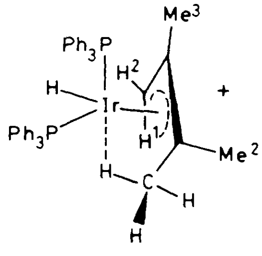

(8)

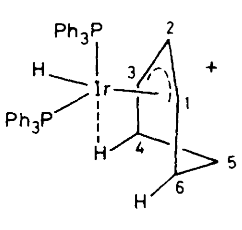

(9)

dihydride to be dominantly (3a), both (3b) and (4) are also observed to form in this reaction at low temperature. These species are best generated by mixing the reactants in an n.m.r. tube at 193 K, warming the tube to *ca.* 273 K for a few seconds then collecting the spectra at 223 K. In this way, sufficient concentrations of the transients are formed with minimal H_2 elimination. The presence of (1), (2), (3a), (3b), and (4) in solution tends to complicate the organic region (*i.e.* δ 0—10 p.p.m.) in the ^1H n.m.r., and therefore the hydride region together with ^{31}P n.m.r. is more informative. Selected n.m.r. data for species (1)—(4) are collected in Table 2.

The rate of interconversion of (3a) to (3b) was not measured although an apparent equilibrium composition (based on hydride and ^{31}P n.m.r. integrals) is *ca.* 3 : 1 for (3a) : (3b) at 223 K. Due to their spectral overlap, only tentative ^1H n.m.r. assignments for bound nbd of (3a) and (3b) are given. Only three transient ^{13}C n.m.r. diene resonances were clearly observed and these are assigned to (3a). The mono-bound *exo*-species (4) is only formed in low concentration, and then only when (1) is present, suggesting a small equilibrium formation constant between (1) and (4). The *endo*-bound structure (**II**, Scheme 1) undergoes rapid chelate ring closure as discussed previously, and this is not possible for the *exo*-bound structure (4). Furthermore, nbe is known to bind in an *exo*-fashion and is hydrogenated exclusively at the *exo*-face by $[Rh(PR_3)_2(diene)][PF_6]$.[16] It would seem reasonable to expect that nbd can also bind in this manner. This non-productive reaction channel will have minimal effect on the s.f.n.m.r. results, as the binding of monoenes to (1) is known to be a thermodynamically unfavourable reversible equilibrium.[7]

The third nbd diene-dihydride isomer (3c) may be generated *in situ* by flushing a dichloromethane solution of (2) with H_2 at 213 K as described for $[Ir(PPh_3)_2(cod)]^+$.[4] The two distinct hydride resonances observed for (3c), and the ^{31}P n.m.r., allow its complete stereochemical assignment. Unlike its cod analogue, (3c) will partially interconvert to (3a) and (3b) on warming (as shown in Figure 3), before H_2 elimination occurs

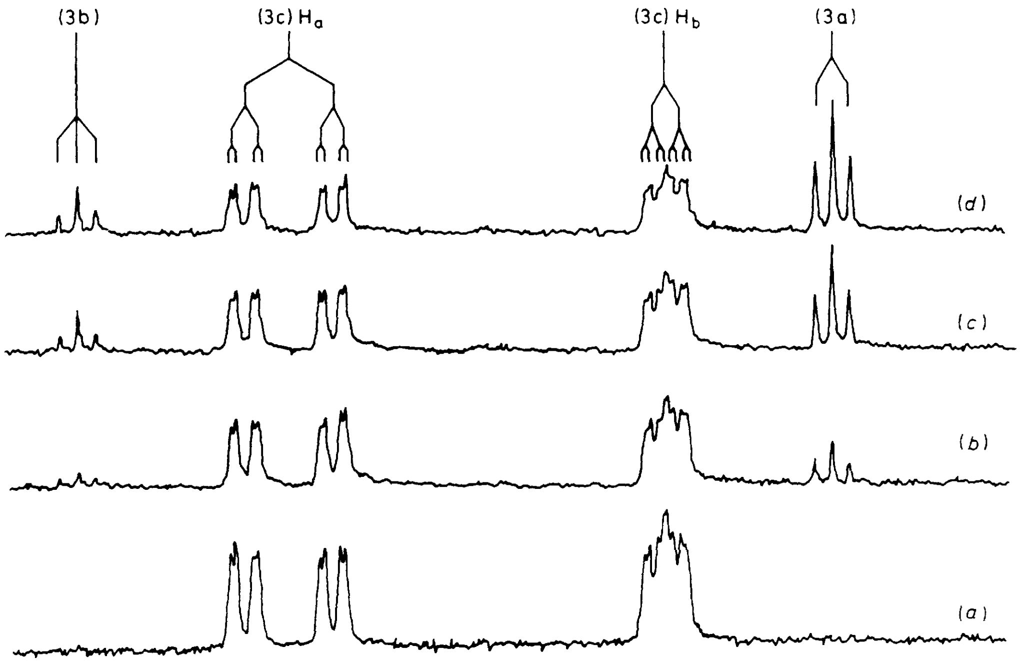

Figure 3. Hydride region in successive [(*a*)—(*d*)] 90-MHz ^1H n.m.r. spectra showing the interconversion of the three isomers of $[Ir(PPh_3)_2(nbd)H_2]^+$ (3a)—(3c). All spectra were taken at 213 K in CD_2Cl_2. Spectrum (*d*): (3a), δ −15.9 p.p.m. ($^2J_{PH}$ = 16.5 Hz); (3b), −7.7 ($^2J_{PH}$ = 17.6); (3c), H_a −10.1 [$^2J_{PH}$ = 84.7 (*trans*) and 21.5 (*cis*), $^2J_{HH}$ = 5.5], H_b −14.2 ($^2J_{PH}$ = 22.3 and 13.4, $^2J_{HH}$ = 5.5)

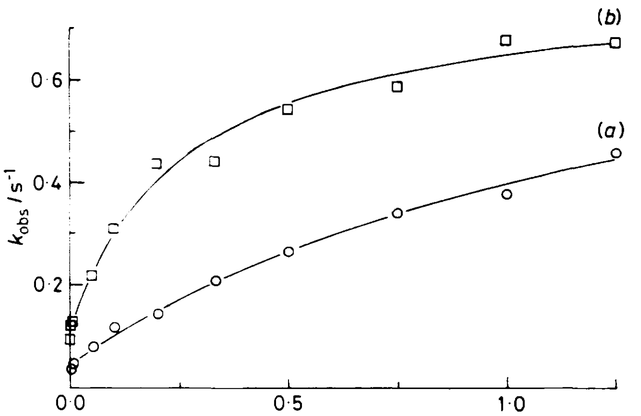

Figure 4. Observed rate constants, $k_{obs.}$, for the formation of $[Ir(PPh_3)_2(nbd)]^+$ (2) from either (*a*) $[Ir(PPh_3)_2(OCMe_2)_2H_2]^+$ (1), or (*b*) $[Ir(PPh_3)_2(OCMe_2)_2D_2]^+$ (5×10^{-4} mol dm^{-3}) with varying nbd concentration in CH_2Cl_2 (+2% v/v Me_2CO) at 298.2 K

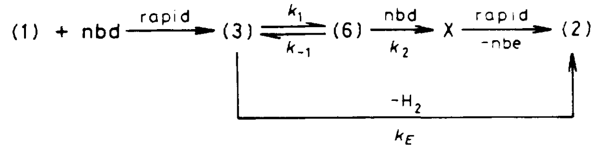

Scheme 2.

Table 3. Rate constants and rate ratios from a non-linear least-squares analysis of the formation of $[Ir(PPh_3)_2(nbd)]^+$ (2) at 298.2 K, according to equation (v). The superscripts H and D refer to hydride and deuteride, respectively

$k_1^H = 0.889 \pm 0.129$ s^{-1}
$(k_{-1}^H/k_2^H) = 1.54 \pm 0.38$ mol dm^{-3}
$k_E^H = (4.60 \pm 0.74) \times 10^{-2}$ s^{-1}
$k_1^D = 0.675 \pm 0.039$ s^{-1}
$(k_{-1}^D/k_2^D) = 0.268 \pm 0.054$ mol dm^{-3}
$k_E^D = 0.114 \pm 0.016$ s^{-1}

to reform (2). It is interesting to note that the ratio (3a) to (3b) formed in this way is again *ca.* 3 : 1. Octahedral iridium(III) species tend to be stereochemically rigid, and it is doubtful that isomer interchange occurs by a pseudorotational process. A more likely pathway for this interconversion would involve a five-co-ordinate species where rapid intramolecular rearrangements are well known.[17] A five-co-ordinate species may be attained either by loss of a ligand (phosphine or proton), or by reversible hydrogen transfer to form an alkyl-hydride species, (6). Since hydrogenation, isomerisation, and cycloalkane-activation reactions occur readily at the bis(phosphine)iridium(III) moiety, then reversible hydrogen transfer between metal and co-ordinated nbd is thought to be the more likely process. Dihydrogen elimination, rather than deprotonation, appears to be the rule in dihydridoiridium(III) chemistry, although deprotonation equilibria have been demonstrated with the analogous rhodium species.[18] At present there is no strong evidence for PPh_3 exchange on these bis(phosphine)iridium systems. All of the diene-dihydride isomers would appear to give sharp ^{31}P n.m.r. resonances.

Kinetic evidence for the alkyl-hydride intermediate (6) was obtained by a single-wavelenth s.f. spectrophotometric study at 298.2 K. The formation of (2) was monitored at 510 and 605 nm in CH_2Cl_2 (+2% v/v Me_2CO) during the reaction of nbd with (1), or its dideuteride $[^2H_2]$-(1). Activation parameters for acetone exchange at $[^2H_2]$-(1) have been measured[9] and are within experimental error of those for (1). The rate constants for acetone exchange at 298.2 K for (1) and $[^2H_2]$-(1) are 395 ± 7 and 385 ± 11 s^{-1}, respectively. Using a fixed concentration of metal (5×10^{-4} mol dm^{-3}) with nbd varied from 4×10^{-4} to 1.25 mol dm^{-3}, the formation of (2) was found to be first order over this entire concentration range. The observed rate constants ($k_{obs.}$) for the formation of (2) are larger for the deuteride compared with the hydride of (1) over the range studied, as shown in Figure 4. In addition, $k_{obs.}$ is dependent on [nbd] showing saturation kinetics. The apparent anomaly of an inverse kinetic isotope effect may be rationalised by proposing the alkyl-hydride complex (6) in the reaction mechanism shown in Scheme 2.

The mechanism for the formation of (2) involves both hydrogenation (k_1,k_2) and H_2 elimination (k_E) pathways. Since there is clearly a significant difference in $k_{obs.}$ for (1) and $[^2H_2]$-(1), it is unlikely that nbd binding is rate determining even though acetone (0.27 mol dm^{-3}) is present to retard the ligand binding process. The observation by n.m.r. of diene-dihydrides as the majority solution species at low temperatures suggests that hydrogen transfer to form (6) (*i.e.* k_1) is the rate-determining step. An equilibrium between (3) and (6) would allow for the interchange of the diene-dihydride isomers as discussed above. The interception of (6) by a further nbd molecule would then be expected to show a rate dependence on free diene. Thus, using a steady-state treatment for (6) in Scheme 2 gives equation (v).

$$k_{obs.} = k_E + \frac{k_1k_2[\mathrm{nbd}]_{free}}{k_{-1} + k_2[\mathrm{nbd}]_{free}} \qquad \text{(v)}$$

Using non-linear least-squares analysis to fit values of $k_{obs.}$ and $[\mathrm{nbd}]_{free}$ to equation(v) gives the rate constants shown in Table 3. If it is assumed that the interception of (6) by nbd is isotope independent (*i.e.* $k_2^H \simeq k_2^D$), then this gives the isotope ratios of equations (vi)—(viii).

$$k_1^H/k_1^D = 1.32 \pm 0.16 \qquad \text{(vi)}$$

$$k_{-1}^H/k_{-1}^D = 5.73 \pm 0.32 \qquad \text{(vii)}$$

$$k_E^H/k_E^D = 0.405 \pm 0.215 \qquad \text{(viii)}$$

The observed inverse kinetic isotope effect is attributed to the large isotope ratio for the k_{-1} step [equation (vii)] in the equilibrium between (3) and (6). Inverse kinetic isotope effects have been noted in other metal-catalysed alkene hydrogenation reactions,[19] although saturation kinetics were not observed as in the present case. The dependence of the k_2 step on [nbd] may well have implication in a catalytic cycle where free substrate could assist the hydrogenation of bound substrate. The species X in Scheme 2 may have a number of possible structures, one of which is shown, (7). This has both alkyl and hydride groups in *cis* positions prior to reductive elimination of nbe, and its structure is comparable to (3c). Elimination of nbe is likely to be *ca.* 10^3 times more rapid than H_2 elimination based on rates measured for CH_4 and H_2 in another study.[20] The reductive elimination of CH_4 from *cis*-$[Pt(PPh_3)_2(Me)H]$, or its deuteride analogue, shows a normal kinetic isotope effect of $k^H/k^D = 3.3$.[21] It is unlikely, therefore, that the reductive elimination of nbe would be slower in the reaction of $[^2H_2]$-(1) compared with (1). In the case of the reaction of cod with (1), the rate of hydrogenation (k_1,k_2 pathway) is much

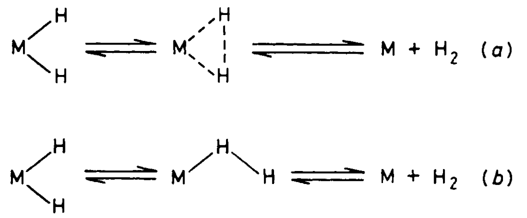

Scheme 3.

slower than the H_2 elimination (k_E pathway). This may be a consequence of cod being a poorer chelating ligand compared to nbd, and cod may not be able to intercept and eventually chelate to the alkyl–hydride intermediate as readily. Hence the H_2 elimination pathway dominates.

Although prone to greater error, there would also appear to be an inverse, kinetic isotope effect for the k_E pathway [equation (viii)]. Two possible mechanisms for this reaction are shown in Scheme 3. Should zero-point energy differences be greater for the three-centre transition state compared to the ground state [Scheme 3(*a*)], then an inverse kinetic isotope effect might be expected. However, the brief existence of an end-on M–H–H intermediate [Scheme 3(*b*)] with a large kinetic isotope effect for a rapid back reaction could also account for this observation. Unfortunately, we have no further supporting evidence for either mechanism. Whether (2) is formed entirely by H_2 elimination from (3c) is also unclear, but this isomer would require the least amount of ligand rearrangement. Dihydrogen loss from (3a) could also be envisaged, but definitely not for (3b).

N.M.R. Evidence for Fluxional Allyl–Hydride Species featuring Aliphatic C–H ⋯ Ir^{III} *Interactions.*—In contrast to the expected diene–dihydride species, the addition of conjugated dienes to (1) in CD_2Cl_2 forms novel fluxional η^3-allyl–hydride species. Two of these systems have been characterised in detail and are discussed in turn.

The reaction of (1) with 2,3-dimethylbutadiene in CD_2Cl_2 gives the fluxional pseudo-octahedral $[Ir(PPh_3)_2\{\eta^3\text{-}CH_2{=}C(Me)CMe_2\}H]^+$ ion (8).[12] The ^1H n.m.r. spectrum of (8) at 253 K consists of a complex phenyl region (30 H), three methyl singlets at δ 2.39 (3 H, Me^2), 1.62 (3 H, Me^3), and −2.23 (3 H, Me^1), two allyl singlets at δ 2.88 (1 H, H^2) and 0.48 (1 H, H^1), and a triplet assigned to the iridium hydride at δ −24.65 p.p.m. (1 H, $^2J_{PH}$ = 18.7 Hz). The unusual Me^1 shift (δ −2.23) is consistent with a C–H ⋯ Ir^{III} interaction, rapid methyl rotation averaging both bridging and terminal C–H shifts. This rotation could not be ' frozen out ' in the low temperature 400-MHz ^1H spectra, although considerable broadening occurs by 153 K in CD_2Cl_2–$CFCl_3$ ($w_{\frac{1}{2}} \simeq$ 280 Hz). This interpretation of the upfield methyl resonance is supported by the observation of three Me^1 resonances for (8) derived from $[^2H_2]$-(1)[13] at δ −2.23, −2.54, and −2.91 assigned to $-CH_3$, $-CH_2D$, and $-CHD_2$, respectively. Anomalously large shifts on deuteriation have been noted in other systems where C–H ⋯ metal interactions occur.[22] [26] These originate from zero-point energy differences where an excess of H over D resides in the bridging position (see Appendix 2). This is complemented by a corresponding shift to lower field for $-CH_2D$ and $-CHD_2$ to δ −1.71 (br, s, Me^1) in the 61.4-MHz ^2H n.m.r. spectrum of (8) at 253 K.

Above 233 K, the allyl and hydride resonances of (8) broaden with the eventual collapse of the hydride signal by 273 K, while Me^2 and Me^3 clearly coalesce by 298 K (δ 2.01). The results of ^1H spin-saturation transfer experiments at 258 K are shown in Figure 5. Irradiation of Me^1 causes significant intensity reduction of H^1, H^2, and Ir–H signals [spectrum 5(*b*)], but not the Me^2 or Me^3 signals, while irradiation of Me^2 [spectrum 5(*c*)] selectively removes Me^3 and *vice versa*. The difference spectrum (*d*) [*i.e.* (*c*) − (*b*)] clearly shows the two unique sets of interconverting protons. Such observations are consistent with a predominant fluxional process at 258 K involving a diene–dihydride intermediate (Scheme 4) analogous to that found for cod and nbd.

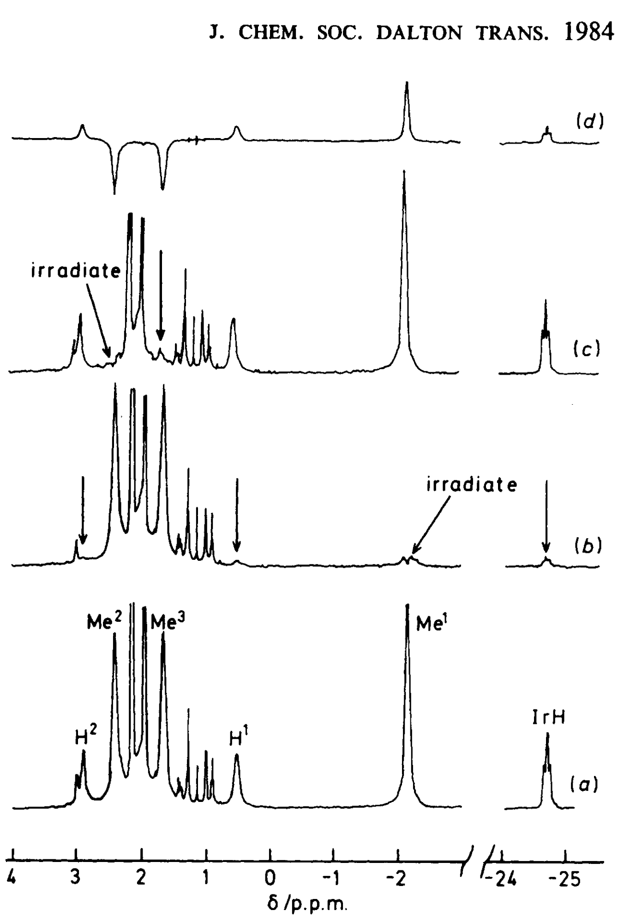

Figure 5. Spin-saturation transfer n.m.r. experiments (^1H, 400 MHz) on $[Ir(PPh_3)_2\{\eta^3\text{-}CH_2{=}C(Me)CMe_2\}H]^+$ (8), formed *in situ* from (1) and excess 2,3-dimethylbutadiene, in CD_2Cl_2 at 258 K. Resonances at δ 2.16 and 1.95 p.p.m. arise from Me_2CO and excess diene, respectively. The other resonances in the range δ 0.8—1.5 p.p.m. arise from traces of light petroleum in the crystalline solid of (1)

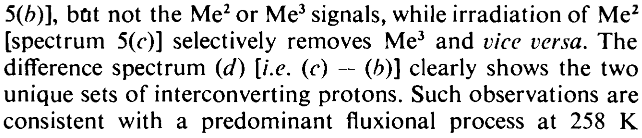

Scheme 4.

To allow for the incorporation of two deuterium atoms at Me^1, either H^a or H^b must be able to transfer to the same terminal carbon atom in the diene–dihydride intermediate (Scheme 4). This is seen more clearly in the spin-saturation transfer experiments for (9) in Figure 6. Variable-temperature 162-MHz ^{31}P n.m.r. spectra reveal two broad resonances of equal intensity at δ 10.5 and 8.2 p.p.m. below 253 K with no $^2J_{PP}$ coupling evident. These resonances coalesce by 298 K. The absence of coupling suggests another fluxional process

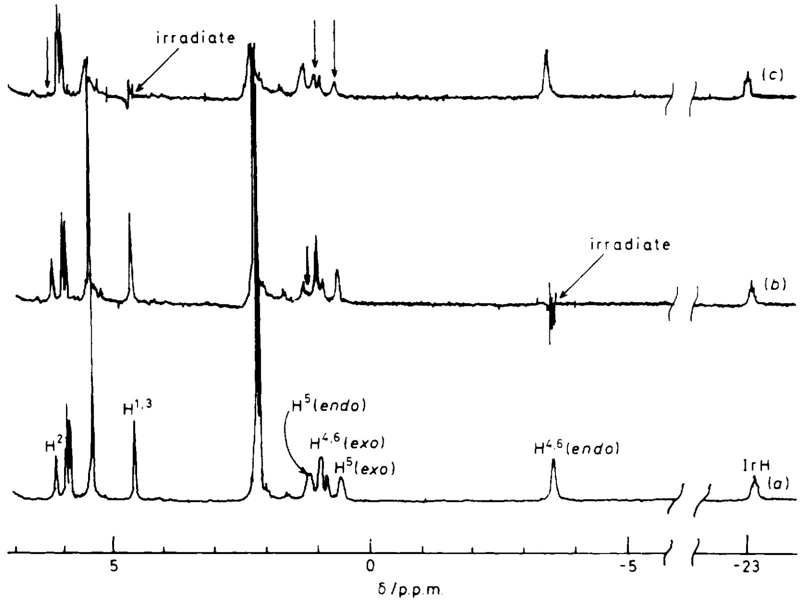

Figure 6. Spin-saturation transfer n.m.r. experiments (^{1}H, 400 MHz) on $[Ir(PPh_3)_2(\eta^3\text{-}C_6H_9)H]^+$ (9), formed *in situ* from (1) and excess cyclohexa-1,3-diene, in CD_2Cl_2 at 213 K. Unlabelled resonances arise from Me_2CO, excess diene and the phenyl protons of (9). Small impurity peaks in the range δ 0.8—1.5 p.p.m. arise from traces of light petroleum in the crystalline solid of (1)

which is likely to be rapid facial rotation of the allyl-Me^1 group about the pseudo-octahedral metal centre. Below 253 K where the hydrogen transfer process becomes slow, the allyl-Me^1 group will become ' locked ' in one of two possible enantiomers. This being the case, the two phosphorus atoms become diastereotopic. Facial rotation of the allyl-Me^1 group will not render the diastereotopic P atoms equivalent, but the onset of rapid H atom transfer above 253 K will do so.

The addition of cyclohexa-1,3- or -1,4-diene to (1) in CD_2Cl_2 forms the $[Ir(PPh_3)_2(\eta^3\text{-cyclohexenyl})H]^+$ ion, (9). This species is also highly fluxional adopting a pseudo-octahedral configuration *via* an aliphatic $C-H\cdots Ir^{III}$ interaction. The ^{1}H n.m.r. spectrum of (9) at 213 K (Figure 6) consists of a complex phenyl region (30 H), two allyl singlets at δ 6.05 (1 H, H^2), 4.54 (2 H, $H^{1,3}$), four broad aliphatic singlets at δ 1.15 (1 H, *endo* H^5), 0.93 (2 H, *exo* H^4, *exo* H^6), 0.54 (1 H, *exo* H^5), and −3.57 (2 H, *endo* H^4, *endo* H^6) and a triplet for the iridium hydride at δ −23.27 p.p.m. [$^2J_{PH}(cis)$ = 18.7 Hz]. Rapid interchange of the H^4 and H^6 *endo* protons in the $C-H\cdots Ir^{III}$ site results in considerable spectral simplification. Thus, both of these protons are in the n.m.r. fast-exchange region at the unusual high-field shift. This process will also cause the H^4 and H^6 *exo* protons to be equivalent and also the H^1 and H^3 allyl protons. An attempt to ' freeze-out ' the process and give the ' locked ' enantiomers proved unsuccessful even at 173 K. The ^{31}P spectra gave a singlet at δ 9.2 over the same temperature range. Since the two phosphorus atoms cannot be diastereotopic in this particular case, the single ^{31}P resonance is taken as further evidence for the rapid facial rotation of the hydrocarbon ligands in both (8) and (9).

When (9) is prepared from $[^2H_2]$-(1), two separate resonances of the H^4 and H^6 *endo* protons result at δ −3.57 and −4.61 p.p.m. The presence of one deuterium atom in the two bridging sites causes the large upfield shift (*i.e.* 1.04 p.p.m.) as was noted with (8) and again is a result of zero-point energy difference (Appendix 2).

Variable-temperature ^{1}H n.m.r. and ^{1}H spin-saturation transfer experiments (213 K) with (9) reveal two unique sets of interchanging protons. The first set contains the hydride and three *endo* protons while the second set contains three *exo* and three allyl protons. The first set can migrate reversibly between carbon and iridium *via* the $C-H\cdots Ir^{III}$ interaction, while each proton of the second set remains firmly anchored to one carbon. At 233 K and above, the hydrocarbon and hydride resonances all broaden. At 263 K, a broad peak appears at δ −1.93 (calculated average shift −1.99) which corresponds to the coalesced *endo* protons. This signal broadens and shifts upfield at higher temperatures when hydride exchange with the *endo* protons becomes dominant. The appearance at 293 K of a broad peak at δ 3.04 (calculated average shift 3.01) confirms the coalescence of the *exo* and allyl protons. Irradiation of the H^4 and H^6 *endo* proton resonance at 213 K [see Figure 6(*b*)] causes a significant intensity reduction at the H^5 *endo* proton site while the hydride remains unaffected. Irradiation of the H^1 and H^3 allyl proton resonance, at the same temperature, causes intensity reductions at the H^2 allyl and H^4, H^5, and H^6 *exo* protons [Figure 6(*c*)]. These results are entirely consistent with an overall 1,4-hydrogen shift on the carbocycle ligand *via* a diene–dihydride intermediate as shown in Scheme 5. The hydride ligand H^a is a spectator to this process at 213 K although it does become involved at higher temperatures (263 K) where signal broadening occurs. The overall effect of this process is to circulate the allyl moiety around the carbocycle framework.

Attempts to isolate (8) and (9) as pure crystalline solids with the exclusion of decomposition products were unsuccessful. In the case of (9), one of the products is $[Ir(PPh_3)_2(\eta^5\text{-}C_6H_7)H][PF_6]$.[5] No $C-H\cdots Ir^{III}$ stretch could be observed for (8) or (9) from solution (CD_2Cl_2) i.r. spectroscopy in the expected 2 500—2 700 cm^{-1} region.[27]

The species $[Fe\{P(OMe)_3\}_3(\eta^3\text{-allyl})][PF_6]$ [23] and $[Mn(CO)_3(\eta^3\text{-}C_6H_9)]$ [24] also have a $C-H\cdots M$ interaction similar to (8) and (9). In the absence of this interaction, each of these species is formally a 16-electron system. The 18-electron configuration is approached by electron delocalisation from the C–H bond to the metal.

Although many examples of reversible hydrogen transfer to

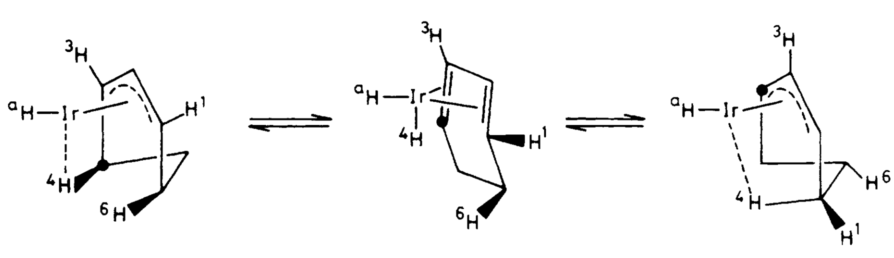

Scheme 5.

hydrocarbon ligands[28] and C–H · · · M interaction[22–27,29] have been reported, they rarely involve catalytically active systems. The possible involvement of a C–H · · · M interaction prior to C–H activation has been discussed. The ion (1) is known to be an alkene isomerisation and hydrogenation catalyst and can activate cycloalkanes. The identification of the C–H · · · Ir^{III} interaction in (8) and (9) may therefore be viewed as an example of a partially hydrogenated diene, or alternatively, as an incipient C–H bond activation. The ^1H spin-saturation transfer experiments clearly show the reversible passage of hydrogen, between metal and hydrocarbon, occurs *via* this interaction. The introduction of deuterium into such reversible hydrogen transfer equilibria clearly has profound effects on C–H · · · M n.m.r. shifts and also on alkene hydrogenation reaction rates.

Experimental

$[Ir(PPh_3)_2(OCMe_2)_2H_2][PF_6]$ (1) was prepared as previously described.[3,7] The dideuteride $[^2H_2]$-(1) was also prepared by the same procedure using D_2 gas {(1), ν(IrH) = 2 250 cm^{-1}; $[^2H_2]$-(1), ν(IrD) = 1 607 cm^{-1}; ν(IrH)/ν(IrD) = 1.4}. These compounds crystallise from acetone–light petroleum (b.p. 40—60 °C) with approximately one molecule of free acetone, and less if placed *in vacuo* for extended periods.

The monoene and diene ligands, cyclo-octa-1,5-diene (cod) cyclo-octene, bicyclo[2.2.1]hepta-2,5-diene (nbd), bicyclo-[2.2.1]hept-2-ene (nbe), cyclohexa-1,3-diene, cyclohexa-1,4-diene, and 2,3-dimethylbutadiene, were used as supplied although all were checked for purity by ^1H and ^{13}C n.m.r. prior to use.

Perkin-Elmer R34 (220 MHz, ^1H), Bruker WH 90 (90 MHz, ^1H; 22.63 MHz, ^{13}C; 36.43 MHz, ^{31}P), and Bruker WH 400 (400 MHz, ^1H; 100.63 MHz, ^{13}C; 162 MHz, ^{31}P; 61.4 MHz, ^2H) spectrometers were used to record n.m.r. spectra. The ^{13}C and ^{31}P spectra were recorded with proton-noise decoupling in all cases. I.r. spectra were recorded with a Perkin-Elmer 580 B instrument.

Stopped-flow n.m.r. and single-wavelength u.v.–visible stopped-flow data (298.2 ± 0.2 K) were obtained with apparatus described previously.[12] Fisons ' Specpure ' CH_2Cl_2 (+2% v/v acetone) A.R. solvent was used in the u.v.–visible study. Stopped-flow traces were fitted by non-linear least-squares regression using an ALGOL program, SFPROG.[30]

Appendix

1. *Kinetic Treatment of S.F.N.M.R. Data for Diene Binding to* (1) (*Scheme* 1).—Applying the steady-state approximation to the intermediates I and II in Scheme 1 gives equations (A1) and (A2) respectively. Eliminating [I] from these two equations gives equation (A3). Therefore, since equation (A4) applies, equation (A5) follows. This leads to equations (i) and (ii) in the text.

$$k_1[MS_2] + k_{-2}[II] = (k_2[\text{diene}] + k_{-1}[S])[I] \quad (A1)$$

$$k_2[\text{diene}][I] = (k_3 + k_{-2})[II] \quad (A2)$$

$$[II] = \frac{k_1k_2[MS_2][\text{diene}]}{k_{-1}[S](k_{-2} + k_3) + k_2k_3[\text{diene}]} \quad (A3)$$

$$-d[MS_2]/dt = \text{rate of formation of product} = k_3[II] \quad (A4)$$

$$-\frac{d[MS_2]}{dt} = \frac{k_1k_2k_3[MS_2][\text{diene}]}{k_{-1}[S](k_{-2} + k_3) + k_2k_3[\text{diene}]} \quad (A5)$$

If the initial concentrations after mixing (*i.e.* time $t = 0$) are [(1)] = a, [diene] = b, and [acetone] = c mol dm^{-3}, and at time t, [(1)] = $(a - x)$, [diene] = $(b - x)$ and [acetone] = $(2x + c)$ mol dm^{-3}, equation (i) may be rewritten as equation (A6). Integration of equation (A6) with the constraint that $x = 0$ at $t = 0$ gives equation (A7).

In this form, the complete l.h.s. of equation (A8) may be considered as a Y-function and the term in square brackets on the r.h.s. as the X-function: equation (A9). Since $(a - x)$ is determined from the integrals of the bound acetone resonance during the course of the s.f.n.m.r. reaction, then $(b - x)$ may also be evaluated. A linear least-squares plot (see Figure 2) will give a gradient of A and an intercept of zero. For nbd, the initial concentrations were $a = 2.45 \times 10^{-2}$, $b = 7.6 \times 10^{-2}$, and $c = 6.7 \times 10^{-3}$ mol dm^{-3}. An unweighted linear least-squares fit gave $A = 0.578 \pm 0.016$ and an intercept of $(3.41 \pm 12.28) \times 10^{-3}$ (*i.e.* zero within experimental error). The concentrations for cod were $a = 2.5 \times 10^{-2}$, $b = 0.25$, and $c = 1.3 \times 10^{-2}$ mol dm^{-3}. A similar analysis for cod gave $A = (5.96 \pm 0.37) \times 10^{-4}$ and an intercept of $(3.62 \pm 2.54) \times 10^{-3}$. The value of k_1 was set at 0.153 s^{-1} in both data analyses.

$$\frac{dx}{dt} = \frac{k_1A(a - x)(b - x)}{(2x + c) + A(b - x)} \quad (A6)$$

$$\{c \ln[b(a - x)/a(b - x)] + 2a \ln(1 - \tfrac{x}{a}) - 2b \ln(1 - \tfrac{x}{b})\}/(a - b) = A[\ln(1 - \tfrac{x}{a}) + k_1t] \quad (A7)$$

$$\frac{c}{a - b}\left[\ln\frac{b(a - x)}{a(b - x)}\right] + \frac{2}{(a - b)}\left[a \ln\frac{a - x}{a} - b \ln\frac{b - x}{b}\right] = A\left[\ln\frac{(a - x)}{a} + k_1t\right] \quad (A8)$$

$$Y = AX \quad (A9)$$

2. *Origin of Chemical Shift Differences upon Deuteriation.*—The energy level diagram for bridging and terminal C–H and

C–D bonds in intermediates of type (8) and (9) is shown below.

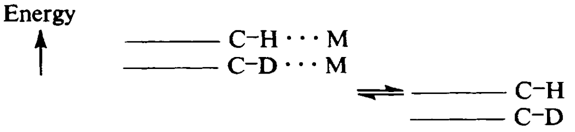

Partial deuteriation of (8) and (9) produces new aliphatic C–H · · · Ir^{III} ^{1}H resonances separated by large chemical shifts. The origin of these shift separations is due to isotope zero-point energy differences. This may be rationalised using (A10) and (A11) to represent the isotope equilibria in (8) and (9), respectively [N.B. two carbon sites are involved in (9)], and a simple four-level energy diagram. The zero-point energy difference will be less for the bridging hydrogen site [typically ν(CH · · · M) ≃ 2 500 cm^{-1}].[27] The relative intensities of the ^{1}H n.m.r. spectra for (8) and (9) would suggest a site preference for deuterium of C–D > C–D · · · Ir > Ir–D. A similar observation was made in another study.[31] A slight energy preference for the C–D bond over the C–H bond will by *default* lead to an excess of H over D in the bridging sites, *i.e.* $K > 1$ in both (A10) and (A11).

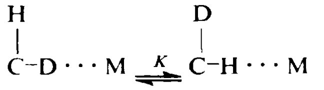
(A10)

$$\overset{\text{H}}{\text{C}}\text{–D}\cdots\text{M} \xrightleftharpoons{K} \overset{\text{D}}{\text{C}}\text{–H}\cdots\text{M} \qquad \text{(A10)}$$

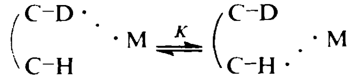
(A11)

The three Me^1 resonances assigned to $^-CH_3$, $^-CH_2D$, and $^-CHD_2$ in (8) may be treated according to equations (A12)—(A15) presented by Calvert and Shapley.[22] The terms δ_b and δ_t are defined as the true chemical shifts for the bridging and terminal methyl hydrogen atoms, respectively (N.B. the terminal hydrogens would be diastereotopic, although the shift differences between these two sites would be negligible in comparison to the overall shift difference between δ_b and δ_t), and ΔE is the energy difference between H- and D-bridged forms. The data for (8) at 253 K give $\delta_b = -9.26$, $\delta_t = 1.28$ p.p.m. and $\Delta E = 0.59$ kJ mol^{-1}. Equation (A12) may be rewritten as (A16) where $\delta_{obs.}$ is an observed shift and X is the percentage occupancy of a single atom in the bridging site.

$$\delta(CH_3) = (2\delta_t + \delta_b)/3 \qquad (A12)$$

$$\delta(CH_2D) = (\delta_t + A\delta_t + \delta_b)/(A + 2) \qquad (A13)$$

$$\delta(CHD_2) = (2A\delta_t + \delta_b)/(2A + 1) \qquad (A14)$$

$$A = \exp(-\Delta E/RT) \qquad (A15)$$

$$\delta_{obs.} = \delta_t - (X/100)(\delta_b - \delta_t) \qquad (A16)$$

The data for (8) give X values of 33.3, 36.3, and 39.8% for single H atoms in $^-CH_3$, $^-CH_2D$, and $^-CHD_2$, respectively. The calculated ^{2}H n.m.r. shifts are δ −1.60 for $^-CH_2D$ and −1.89 p.p.m. for $^-CHD_2$ which agree favourably with the observed single broad resonance at δ −1.71 p.p.m.

Acknowledgements

We are grateful to Dr. E. H. Curzon for obtaining n.m.r. spectra on the Bruker WH400. We thank Johnson Matthey for a generous loan of iridium trichloride and the S.E.R.C. for financial support.

References

1 R. Crabtree, *Acc. Chem. Res.*, 1979, **12**, 331.
2 R. Crabtree, H. Felkin, and G. E. Morris, *J. Organomet. Chem.*, 1977, **141**, 205.
3 J. R. Shapley, R. R. Schrock, and J. A. Osborn, *J. Am. Chem. Soc.*, 1969, **91**, 2816.
4 R. H. Crabtree, H. Felkin, T. F. Khan, and G. E. Morris, *J. Organomet. Chem.*, 1979, **168**, 183.
5 R. H. Crabtree, M. F. Mellea, J. M. Mihelcic, and J. M. Quirk, *J. Am. Chem. Soc.*, 1982, **104**, 107.
6 D. Baudry, M. Ephritikhine, and H. Felkin, *J. Chem. Soc., Chem. Commun.*, 1980, 1243: 1982, 606; A. H. Janowicz and R. G. Bergman, *J. Am. Chem. Soc.*, 1982, **104**, 352; J. K. Hoyanan and W. A. G. Graham, *ibid.*, 1982, **104**, 3723.
7 O. W. Howarth, C. H. McAteer, P. Moore, and G. E. Morris, *J. Chem. Soc., Dalton Trans.*, 1981, 1481.
8 O. W. Howarth, C. H. McAteer, P. Moore, G. E. Morris, and N. W. Alcock, *J. Chem. Soc., Dalton Trans.*, 1982, 541.
9 C. H. McAteer, Ph.D. Thesis, University of Warwick, 1981.
10 A. J. Brown, O. W. Howarth, P. Moore, and W. J. E. Parr, *J. Chem. Soc., Dalton Trans.*, 1979, 1776.
11 A. J. Brown, Ph.D. Thesis, University of Warwick, 1977.
12 P. Moore, *Chimia*, 1979, **33**, 335.
13 O. W. Howarth, C. H. McAteer, P. Moore, and G. E. Morris, *J. Chem. Soc., Chem. Commun.*, 1981, 506.
14 O. W. Howarth, C. H. McAteer, P. Moore, and G. E. Morris, *J. Chem. Soc., Chem. Commun.*, 1982, 745.
15 N. H. Werstiuk, *Can. J. Chem.*, 1970, **48**, 2310.
16 R. R. Schrock and J. A. Osborn, *J. Am. Chem. Soc.*, 1976, **98**, 4450.
17 J. R. Shapley and J. A. Osborn, *Acc. Chem. Res.*, 1973, **6**, 305.
18 R. R. Schrock and J. A. Osborn, *J. Am. Chem. Soc.*, 1976, **98**, 2134.
19 R. L. Sweany and J. Halpern, *J. Am. Chem. Soc.*, 1977, **99**, 8335; J. P. Collman, R. G. Finke, P. L. Matlock, P. Wahren, R. G. Komoto, and J. I. Brauman, *ibid.*, 1978, **100**, 1119; J. A. Roth and M. Orchin, *J. Organomet. Chem.*, 1979, **182**, 299; R. Sweany, S. C. Butler, and J. Halpern, *ibid.*, 1981, **213**, 487; R. L. Sweany, D. S. Comberrel, M. F. Dombourian, and N. A. Peters, *ibid.*, 1981, **216**, 57.
20 E. L. Muetterties and P. L. Watson, *J. Am. Chem. Soc.*, 1978, **100**, 6978.
21 L. Abis, A. Sen, and J. Halpern, *J. Am. Chem. Soc.*, 1978, **100**, 2915.
22 R. B. Calvert and J. R. Shapley, *J. Am. Chem. Soc.*, 1978, **100**, 7726.
23 S. D. Ittel, F. A. Van-Catledge, and J. P. Jesson, *J. Am. Chem. Soc.*, 1979, **101**, 6905.
24 M. Brookhart, W. Lamanna, and M. B. Humphrey, *J. Am. Chem. Soc.*, 1982, **104**, 2117.
25 C. P. Casey, P. J. Fagan, and W. H. Miles, *J. Am. Chem. Soc.*, 1982, **104**, 1134.
26 G. M. Dawkins, M. Green, A. G. Orpen, and F. G. A. Stone, *J. Chem. Soc., Chem. Commun.*, 1982, 41.
27 S. Trofimenko, *J. Am. Chem. Soc.*, 1968, **90**, 4754; *Inorg. Chem.*, 1970, **9**, 2493.
28 J. W. Byrne, H. U. Blaser, and J. A. Osborn, *J. Am. Chem. Soc.*, 1975, **97**, 3871; R. B. Calvert and J. R. Shapley, *ibid.*, 1977, **99**, 5225; C. Crocker, R. J. Errington, W. S. McDonald, K. J. Odell, B. L. Shaw, and R. J. Goodfellow, *J. Chem. Soc., Chem. Commun.*, 1979, 498; R. B. A. Pardy, M. J. Taylor, E. C. Constable, J. D. Mersh, and J. K. M. Sanders, *J. Organomet. Chem.*, 1982, **231**, C25; J. D. Fellman, R. R. Schrock, and D. D. Traficante, *Organometallics*, 1982, **1**, 481 and refs. therein.
29 D. M. Roe, P. M. Bailey, K. Moseley, and P. M. Maitlis, *J. Chem. Soc., Chem. Commun.*, 1972, 1273; F. A. Cotton, T. LaCour, and A. G. Stanislowski; *J. Am. Chem. Soc.*, 1974, **96**, 754; F. A. Cotton and V. W. Day, *J. Chem. Soc., Chem. Commun.*, 1974, 415; M. Pasquoli, C. Floriani, A. G. Manfredott, and A. C. Villa, *J. Am. Chem. Soc.*, 1978, **100**, 4918; A. J.

Schultz, J. M. Williams, R. R. Schrock, G. A. Rupprecht, and J. D. Fellman, *ibid.*, 1979, **101**, 1593; R. K. Brown, J. M. Williams, A. J. Schultz, G. D. Stucky, S. D. Ittel, and R. L. Harlow, *ibid.*, 1980, **102**, 981; A. J. Schultz, R. K. Brown, J. M. Williams, and R. R. Schrock, *ibid.*, 1981, **103**, 169; M. A. Beno, J. M. Williams, M. Tachikawa, and E. L. Muetterties, *ibid.*, 1981, **103**, 1485 and refs. therein.

30 P. Moore, *J. Chem. Soc., Faraday Trans 1*, 1972, 1890.

31 R. B. Calvert, J. R. Shapley, A. J. Schultz, J. M. Williams, S. L. Suib, and G. D. Stucky, *J. Am. Chem. Soc.*, 1978, **100**, 6240.

Received 28th July 1983; *Paper* 3/1315